Available online at www.sciencedirect.com
SCIENCE DIRECT
Journal of Physics and Chemistry of Solids 67 (2006) 516–521
JOURNAL OF PHYSICS AND CHEMISTRY OF SOLIDS
www.elsevier.com/locate/jpcs

Strong coupling superconductivity via an asymptotically exact renormalization-group framework

S.-W. Tsai [a,*], A.H. Castro Neto [a], R. Shankar [b], D.K. Campbell [a]

[a] *Department of Physics, Boston University, Boston, MA 02215, USA*
[b] *Sloane Laboratory of Physics, Yale University, New Haven, CN 06520, USA*

Abstract

A renormalization-group approach for interacting electrons, which are also coupled to phonons was recently developed [1]. The method is described here in some detail, including the large-N analysis which shows that the theory is asymptotically exact and from which Migdal's theorem follows as a consequence. We present analytical and numerical results for the case of an isotropic Fermi surface and Einstein phonons. In this case Eliashberg's strong coupling theory emerges as the $N \to \infty$ theory. Both $T=0$ and finite-T renormalization-group formalisms are developed.

Electron–electron interactions are responsible for a vast number of striking properties in condensed matter systems. Electrons in solids also interact with bosonic modes, such as phonons. Recently [1] we developed a method that treats electron–electron and electron–phonon interactions on an equal footing. It is a renormalization-group (RG) approach [2], which provides an unbiased way of studying instabilities of Fermi liquids without the assumption of a particular broken symmetry. Experimental evidence shows that in many strongly correlated systems, such as high-temperature superconductors and organic charge-transfer salts, both electron interactions and phonons seem to play an important role [3–8]. Theoretical understanding of the interplay between these interactions is a complex issue. Most theoretical approaches rely on mean-field treatments where a particular order parameter and broken symmetry are introduced 'by hand'. While this is useful in understanding the properties of the particular broken symmetry state, it is desirable to have methods that predict the leading instability given the geometry of the Fermi surface and the microscopic parameters at a high energy scale, when the system is in the disordered Fermi liquid state.

The RG provides such an approach [2], which has been successful in explaining the stability and instabilities of Landau Fermi liquids in more than one dimension. It involves a two-stage procedure. First, given a microscopic theory defined in all of momentum space and with an energy bandwidth of order of E_F, one reduces the energy cut-off to a smaller energy scale $\Lambda_0 \ll E_F$ via mode-elimination. The calculation in this first stage is purely perturbative and can only be carried out within the assumptions of perturbation theory. It is assumed for example that in reducing the energy cut-off from E_F to Λ_0, the new cut-off theory does not run into a non-perturbative singularity in the process.

Once the cut-off scale Λ_0 is reached safely, the second stage consists in further reducing the cut-off to $\Lambda < \Lambda_0$ by using the method of large-N, with $N \simeq E_F/\Lambda$. In $d=2$, which is our focus in this work, the remaining phase space has the form of an annulus of radius K_F (the Fermi momentum) and width $2\Lambda/v_F$ (where v_F is the Fermi velocity). Imagine now dividing the annulus into N patches of size $(\Lambda/2v_F)^2$. The momentum of each fermion $\mathbf{k}$ is a sum of a 'large' part (order k_F) centered on a patch labeled by a patch index $i=1,\ldots N$ and a 'small' momentum (order Λ) within the patch. It can then be verified that in all Feynman diagrams of this cut-off theory the patch index plays the role of a conserved isospin index exactly as in a theory with N fermionic species. In the RG flow equations for the interaction vertices the sum of bubble diagrams are singled out by the $1/N$ expansion and reproduce Landau's Fermi liquid theory for circular Fermi surface and repulsive bare interaction. A central result which also applies in the present work is that starting at the scale Λ_0, the one-loop β-function for the fermion–fermion coupling becomes exact as $\Lambda \to 0$ ($N \to \infty$) via RG.

Here, we present some details of the RG procedure of Ref. [1] which applies to interacting electrons coupled to phonons. We show analytical and numerical results for the case

* Corresponding author. Present address: Department of Physics, University of California, Riverside, CA 92521, USA.
E-mail address: swtsay@bu.edu (S.-W. Tsai).

0022-3697/$ - see front matter © 2005 Elsevier Ltd. All rights reserved.
doi:10.1016/j.jpcs.2005.10.069

of a circular Fermi surface with on-site electron–electron interaction and Eisntein phonons, both at $T=0$ and at finite T. We find that the high-temperature Fermi liquid state becomes unstable toward Cooper pairing at a temperature scale T^*. This temperature is the same as the critical temperature T_c obtained from Eliashberg's strong coupling self-consistent mean field theory. We then discuss the large-N analysis and Migdal's theorem.

1. The RG equations

We work in the path-integral representation and consider the general action

$$S(\psi,\phi) = S_e(\psi) + S_{ph}(\phi) + S_{e-ph}(\psi) + S_{e-e}(\psi) \tag{1}$$

where

$$S_e = \int_{\omega\mathbf{k}} \psi_k^\dagger (i\omega - \varepsilon_{\mathbf{k}})\psi_{\mathbf{k}} \tag{2}$$

and

$$S_{ph} = \int_{\Omega\mathbf{q}} \phi_q^\dagger (i\Omega - w_{\mathbf{q}})\phi_q \tag{3}$$

are the free actions for the electrons and the phonons, respectively. Here $k=\{\omega,k\}$ and $q=\{\Omega,\ q\}$ where ω,Ω are the Matsubara frequencies and $\mathbf{k},\mathbf{q}$ are the momenta. We first focus on $T=0$ and $d=2$ where $\int_{\omega,\mathbf{k}} \equiv \int_{-\infty}^{\infty} \frac{d\omega}{2\pi} \int \frac{d\mathbf{k}}{(2\pi)^2}$. The interaction terms are given by

$$S_{e-ph} = \int_{\omega\mathbf{k}} \int_{\Omega\mathbf{q}} g(q)\psi_{k+q}^\dagger \psi_k (\phi_q + \phi_{-q}^\dagger) \tag{4}$$

and

$$S_{e-e} = \frac{1}{2}\prod_{i=1}^{3} \int_{\omega_i \mathbf{k}_i} u(k_4,k_3,k_2,k_1)\psi_{k_4}^\dagger \psi_{k_3}^\dagger \psi_{k_2}\psi_{k_1} \tag{5}$$

where $k_4 = k_1 + k_2 - k_3$ from conservation of total momentum and frequency. We use units such that $\hbar = 1 = k_B$ throughout the paper. The above action defines the input physics at a cut-off Λ_0 such that $\omega_D \ll \Lambda_0 \ll E_F$, where ω_D is the Debye frequency. In this way at any subsequent scale $\Lambda < \Lambda_0$ we have $N \simeq E_F/\Lambda_0 \gg 1$. The expansion in $1/N$ can then safely be made and the one loop result becomes exact as the RG takes $\Lambda \to 0$, i.e. $N \to \infty$.

The phonons are described by a Gaussian action and can therefore be integrated out exactly leading to the retarded electron–electron interaction given by

$$\tilde{u}(k_4,k_3,k_2,k_1) = u(k_4,k_3,k_2,k_1) - 2g(k_1,k_3)g(k_2,k_4)D(k_1-k_3), \tag{6}$$

where

$$D(q) = \frac{\omega_{\mathbf{q}}}{(\omega^2 + \omega_{\mathbf{q}}^2)}$$

is the phonon propagator.

We now carry out the RG procedure for this retarded interaction $\tilde{u}$, shown schematically in Fig. 1(a).

The couplings depend on the momenta of the incoming and outgoing electrons. Since, $E_F \gg \omega_D, g, u_0$ we ignore radial excursions away from the Fermi surface. In this case the external electron momenta can be put on k_F. Therefore, for a circular Fermi surface, as the energy cut-off is lowered, only two types of interaction vertex remain: forward scattering with $k_1=k_3$, $k_2=k_4$ (these evolve into Landau parameters) and the scattering in the Cooper channel with $k_1=-k_2$, $k_3=-k_4$. The box vertex in the diagrams in Fig. 1 can represent either one of these scattering processes. The forward scattering channel (which does not flow under the RG as in the case of pure electron–electron interactions) contributes to the electron self-energy $\Sigma(\mathbf{k},\omega)$ via the tadpole diagram shown in Fig.1(b). We can write $\Sigma(\omega,\mathbf{k}) \approx \Sigma_0 + i(1-Z(\omega,\mathbf{k}))\omega$ with two types of contributions: a shift in the chemical potential ($\delta\mu \propto \Sigma_0$) and wave-function renormalization, $Z(\omega)$. The shift in the chemical potential comes from the instantaneous part of $\tilde{u}$. It is convenient to reabsorb it in the theory by assuming a fixed number of electrons [2]. There is also wave-function renormalization, $Z(\omega)$, which comes from the retarded potential due to the phonons and is of special interest in this problem.

In Wilson-like RG the high-energy mode elimination is followed by rescaling of all momenta and frequency in order to preserve the non-interacting part of the action. With the wave-function renormalization $Z(\omega)$, the rescaling becomes non-trivial. The fact that rescaling is a problem can be seen even without the calculation of $Z(\omega)$. In the original action there are electrons and phonons, and while electronic momenta scale differently in the directions parallel and perpendicular to the Fermi surface, the phonon momenta scale isotropically. We circumvent this problem by abandoning the momentum rescale procedure altogether. Instead we use the quantum field theory version of the RG in which the cut-off dependence of the couplings are defined by imposing that the physical quantities are preserved [9].

At a given cut-off Λ, the interaction vertex $\Gamma^{(4)}[\tilde{u}]$ in the Cooper channel (see Fig.1(c)) is given at one-loop by

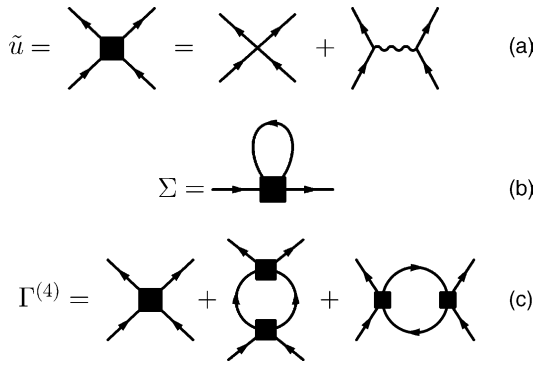

Fig. 1. (a) The solid square represents the retarded electron–electron interaction obtained upon integration of the phonon modes. (b) The tadpole diagram gives contribution to the electron self-energy. (c) Corrections to the interaction vertex, including the diagram at tree level, the BCS and the zero-sound (ZS) contributions.

$$\Gamma^{(4)}[\tilde{u}(-k_3,k_3,-k_1,k_1)]$$
$$= \tilde{u}(-k_3,k_3,-k_1,k_1)$$
$$-\int_{\omega\mathbf{k}} \frac{\tilde{u}(-k,k,-k_1,k_1)\tilde{u}(-k_3,k_3,-k,k)}{(i\omega-\varepsilon_{\mathbf{k}}-\Sigma(\omega,\mathbf{k}))(-i\omega-\varepsilon_{\mathbf{k}}-\Sigma(-\omega,\mathbf{k}))}, \quad (7)$$

where the momentum integral is such that all internal energies lie between 0 and Λ. This is represented by Fig. 1(c), where for the Cooper channel, the BCS diagram contributes and the ZS diagram does not. The RG Eq. for $\tilde{u}$ is obtained from (7) by imposing the condition of cut-off independence, namely, $d\Gamma^{(4)}/d\ell = 0$, where $\ell = ln(\Lambda_0/\Lambda)$ is the RG scale.

For a circular Fermi surface the external electron momenta are vectors of magnitude k_F and $\tilde{u}(-k_3,k_3,-k_1,k_1)$ depends on the angles θ_1 and θ_3 only via the difference $\theta_1-\theta_3$. We can then define s-wave component of $\tilde{u}$

$$\tilde{v}(\omega_1,\omega_3) = N(0)\int\frac{d\theta_1}{2\pi}\int\frac{d\theta_3}{2\pi}\tilde{u}(-k_3,k_3,-k_1,k_1),$$

where $N(0)$ is the Fermi surface density of states.

Imposing now the condition $d\Gamma^{(4)}/d\ell = 0$ on (7) one obtains

$$\frac{d}{d\ell}\tilde{v}(\omega_1,\omega_3,\ell) = -\int_{-\infty}^{\infty}\frac{d\omega}{\pi}\frac{\Lambda_\ell\tilde{v}(\omega_1,\omega,\ell)\tilde{v}(\omega,\omega_3,\ell)}{\Lambda_\ell^2+Z_\ell^2(\omega)\omega^2}, \quad (8)$$

The initial condition is given by

$$\tilde{v}(\omega_1,\omega_3,\ell=0) = u_0-\lambda\omega_E D(\omega_1-\omega_3) \quad (9)$$

where u_0 is the bare electron–electron interaction and λ, for Einstein phonons, is given by $\lambda = 2N(0)g^2/\omega_E$.

We obtain *functional* flow Eq. (8) because retardation introduced by the phonons leads to a mixing of the couplings at low and high frequencies. The RG Eq. for $Z_\ell(\omega)$ is derived from diagram shown in Fig. 1(b). It can then be formally integrated to give

$$Z_\ell(\omega) = 1+\frac{1}{\pi\omega}\int_{-\infty}^{\infty}d\omega'\int_{\Lambda_\ell}^{\infty}d\Lambda'\frac{Z_{\Lambda'}\omega' D(\omega-\omega')}{Z_{\Lambda'}^2(\omega')\omega'^2+\ell\Lambda'^2}. \quad (10)$$

If the frequencies are taken as discrete, the RG Eqs. for the couplings (8) can be written as a matrix equation:

$$\frac{d\mathbf{U}}{d\ell} = -\mathbf{U}\cdot\mathbf{M}\cdot\mathbf{U} \quad (11)$$

where

$$U_{ij}(\ell) = \tilde{v}(\omega_i,\omega_j,\ell),$$

$$M_{ij}(\ell) = \Lambda_\ell\delta_{ij}/\pi(\Lambda_\ell^2+Z_\ell^2(\omega_i)\omega_i^2).$$

The solution of the matrix Eq. (11) is:

$$\mathbf{U}(\ell) = [1+\mathbf{U}(0)\cdot\mathbf{P}(\ell)]^{-1}\mathbf{U}(0),$$

where

$$\mathbf{P}(\ell) = \int_0^\ell d\ell'\mathbf{M}(\ell')$$

and $\mathbf{U}(0)$ is given by the initial condition (9).

An instability is signaled by the divergence of any of the couplings $\tilde{v}(\omega_i,\omega_j,\ell)$ at a certain scale $\ell=\ell_c$. The condition for this to happen is given by

$$\det[1+\mathbf{U}(0)\cdot\mathbf{P}(\ell_c)] = 0. \quad (12)$$

Equivalently ℓ_c is the scale at which an eigenvalue of the matrix $[1+\mathbf{U}(0)\cdot\mathbf{P}(\ell)]$ first becomes zero. Let $\mathbf{f}$ be the corresponding eigenvector, then

$$[1+\mathbf{U}(0)\cdot\mathbf{P}(\ell_c)]\cdot\mathbf{f} = 0.$$

Writing the explicit for of $\mathbf{U}(0)$ and $\mathbf{P}(\ell_c)$ we get

$$f(\omega) = -\frac{1}{\pi}\int_{\omega'}\int_{\Lambda_c}^{\infty}\frac{[u_0-\lambda\omega_E D(\omega-\omega')]}{Z_\Lambda^2(\omega')\omega'^2+\Lambda^2}f(\omega'). \quad (13)$$

For a given value of input parameters (u_0, λ, ω_E, Λ_0) Eq. (13), together with Eq. (10), determine the critical cut-off energy scale, Λ_c, at which the running couplings diverge and the Fermi liquid description breaks down.

2. Finite T

The calculation is readily extended to $T>0$. This provides us with a more experimentally accessible quantity, namely, a critical temperature. We seek the temperature T^* below which the Fermi liquid description breaks down as one scales toward the Fermi surface. In this case we replace the frequency integrals in (10) and (13) by Matsubara sums and extend the integrals in Λ from 0 to ∞ to obtain

$$Z(\omega_n)\phi(\omega_n) = -\pi T^*\sum_m[u_0-\lambda\omega_E D(\omega_n-\omega_m)]\frac{\phi(\omega_m)}{|\omega_m|}, \quad (14)$$

where we have defined $\phi(\omega_n)=f(\omega_n)/Z(\omega_n)$ and $\omega_n = \pi T^*(2n+1)$ (n is an integer). Moreover, from (10) we find:

$$Z(\omega_n) = 1+\lambda\omega_E\frac{\pi T^*}{\omega_n}\sum_m \mathrm{sgn}(\omega_m)D(\omega_n-\omega_m). \quad (15)$$

The solution of (14) and (15) gives the value of T^* as a function of the input parameters. We solve the problem numerically through the following procedure: we first calculate $Z(\omega_n, T)$ for temperatures starting at high values (of the order of Λ_0) and for decreasing values. One could then solve (14), which is self-consistent for $\phi(\omega_n)$, in order to obtain T^*. But, instead, there is a much more straightforward way to calculate T^* which does not involve the self-consistent equation. The relation shown in (14) comes from imposing the condition $\det[1+\mathbf{U}(0)\cdot\mathbf{P}(T^*)]=0$. So instead of solving the self-consistent equation, we simply compute the quantity $\det[1+\mathbf{U}(0)\cdot\mathbf{P}(T)]$ and find out at which temperature it becomes zero (inset of Fig. 2). Calculation of this determinant simply requires knowledge of the initial conditions and the wave-function renormalization $Z(\omega_n T)$. This calculation was repeated for many values of λ as shown in the main plot of Fig. 2. The three solid curves are for different values of the electron interaction, as indicated. For convenience we have expressed the temperatures in units of ω_E.

We now relate our approach to Eliashberg's self-consistent mean-field theory [11,12] which assumes a broken symmetry

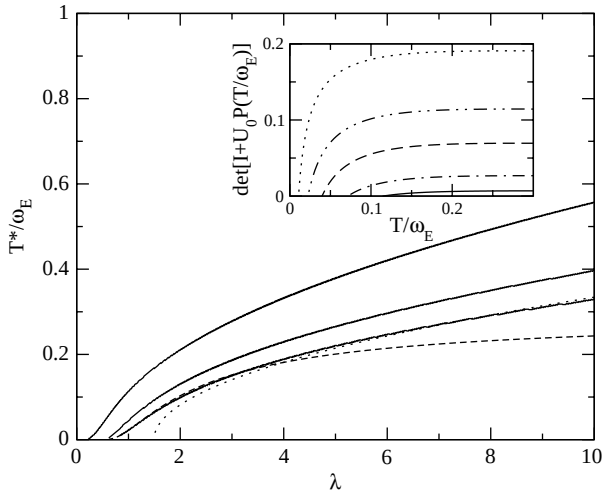

Fig. 2. Numerical solution of (12) (continuous line) for $\mu^*=0$, 0.17, and 0.24 (from top to bottom) as a function of λ. Dashed line: $T^*/\omega_E = 1.1\exp\{-(1+\lambda)/(\lambda+\mu^*(1+\lambda)\}$ for $\mu^*=0.24$; dotted line: $T^*/\omega_E = 0.11\sqrt{\lambda-1.49}$ for $\mu^*=0.24$. The inset shows the determinant in (12) as a function of T for $\mu^*=0$ and $\lambda=0.3$, 0.4, 0.5, 0.7 and 1 (from top to bottom).

with a superconducting order parameter $\Delta(\omega_n)$, in contrast to ours which starts from the Fermi liquid phase. Remarkably (14) and (15) coincide with the Eliashberg equations at $T=T_c$ if we replace $\phi(\omega_n)$ by $\Delta(\omega_n)$ [12]. This result is striking since $\phi(\omega_n)$ is not an order parameter and no symmetry breaking was assumed in our calculation. By the same token, we can show that in the $T=0$ formalism Λ_c plays the role of the zero temperature superconducting gap Δ_0 [10]. Since the RG procedure, approaching the instability from high temperatures, leads to an instability of the Fermi liquid state at a temperature T^* that is equal to the critical temperature T_c produced by the Eliashberg theory, it is no surprise that we can show that in the weak/intermediate coupling regime ($\mu^* < \lambda < 1$) we recover the famous McMillan formula [13]: $T^* \approx 1.13\omega_E \exp\{-(1+\lambda)/(\lambda-\mu^*(1+\lambda))\}$, where $\mu^* = u_0/(1+u_0\, ln(\Lambda_0/\omega_E))$ is the effective electron–electron interaction [14] at the scale of ω_E and the Allen-Dynes expression [15,16]: $T^* \approx 0.16\sqrt{\lambda}\omega_E$ at strong coupling. In addition we have demonstrated that Eliashberg's theory is an asymptotically exact description of the effective low-energy physics obtained by RG thanks to the small parameter $1/N$. For arbitrary shapes of the Fermi surface, the momentum on the Fermi surface can be discretized in angular patches [20] for purposes of numerical computation. Our methods can be used to study the competition between charge density wave and superconductivity in the strong coupling regime [10], something that cannot easily be achieved in a mean-field approach.

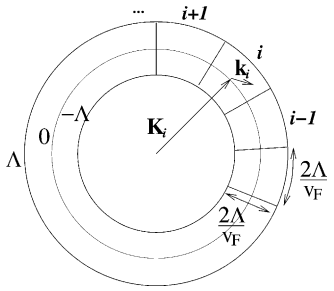

Fig. 3. At an energy cut-off Λ the remaining momentum space is divided in N patches of size $(2\Lambda/v_F)^2$. The patch index plays the hole of a conserved isospin and N is then the number of fermion species.

Since Eliashberg's theory is based on Migdal's theorem [17], which states that electron–phonon vertex corrections to the electron self-energy vanish as $\omega_D/E_F \to 0$, it must be that this theorem is built into our approach. We shall show how this result arises and that the small parameter ω_D/E_F of Migdal's theorem is replaced here by $1/N$.

3. The 1/N picture

The starting point of the RG flow is at energy cut-off of $\Lambda_0 \ll E_F$ such that $N \gg 1$. The $1/N$ picture introduced by Shankar [2] shows that from this point on the RG resummation of diagrams is non-perturbative in the strength of the couplings and asymptotically exact as $N \to \infty$. The idea behind it was briefly summarized in the introduction and illustrated in Fig. 3. While the $1/N$ analysis apply in the same way to the present case where $\tilde{u}$ is frequency-dependent, it is instructive to go back to the problem before we traced out the phonons.

Let's see how the patch index notation carries over to the labeling of the phonons. Electrons and phonons interact via Eq. (4). While it is obvious that when a fermion in patch i scatters to patch j, it emits a phonon of momentum $\mathbf{k}_j - \mathbf{k}_i$, we can also go the other way: a phonon of 'large' momentum can be resolved, up to a two-fold ambiguity, into a difference $\mathbf{k}_i - \mathbf{k}_j$ associated with patches i and j, due to the fact that the electron momenta lie in a thin annulus around the Fermi surface. This fact allows us to describe phonons with the double-index notation employed by t'Hooft for gluons in QCD [18]: the phonon line is seen as made out of two counter-propagating electron lines, as depicted in Fig.4(a). The fermion-fermion interaction scales as $1/N$. Integrating out the phonons produces a four-fermion term which goes as g^2, therefore, the electron–phonon vertex g scales as $1/\sqrt{N}$.

Any given diagram made of n_u vertices u, n_g vertices g and n_L internal loops is of order $(1/N)^n$ where $n = -n_u - n_g/2 + n_L$. Therefore, we can easily organize the perturbation theory in orders of $1/N$. The number of loops in each diagram, n_L, can be easily obtained using the representation of Fig.4(a). Consider the problem of the RG for the self-energy $\Sigma(\mathbf{k},\omega)$ shown in Fig. 4(b)–(d). It is clear from Fig. 4(b) that the correction of order g^2 should be taken into account: while g^2 comes with a factor $1/N$, there is an internal closed loop giving an extra factor of N resulting in a correction of $O(N^0)$ for the self-energy. At the same order in perturbation expansion in $1/N$, there are diagrams that are made from a simple repetition of Fig. 4(b), which are obviously of order $O(N^0)$ but higher order in g. Diagram Fig. 4(c) is of order $O(N^0)$, like diagram 4(b), and so are all the other 'rainbow' diagrams that are automatically included into the theory. Thus, by solving the RG equations for a 'running' self-energy at one-loop, we in fact take into account *all* corrections of order $O(N^0)$ to *all* loops. The infinite series of diagrams being summed is not arbitrary and arises naturally

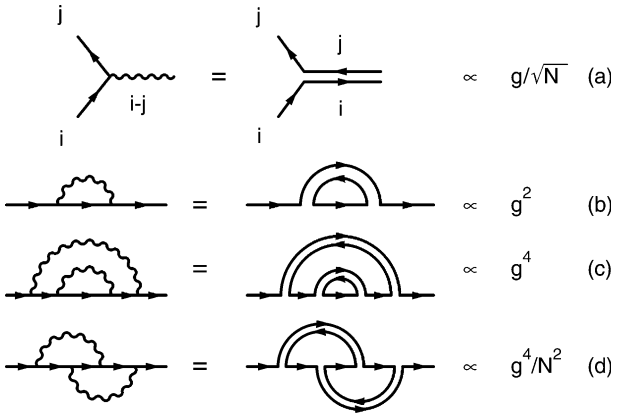

Fig. 4. (a) Electron–phonon interaction vertex and the double index representation of the phonon propagator (a). Contributions to the electron self-energy are shown in (b), (c) and (d) and their corresponding order in the $1/N$ expansion.

from the RG equations, as shown by our $1/N$ analysis. These corrections to the self-energy lead to the wave-function renormalization Z shown in (10). The final diagram of order g^4 is shown in Fig.4(d): this is the famous vertex correction to the electron self-energy due to electron–phonon interactions studied by Migdal [17]. While at first glance it seems to contain closed internal loops, following the propagating solid line in the double-index representation shows that the loop never closes. This diagram 4(d) is, therefore, of order $O(N^{-2})$ and thus vanishingly small as $N\to\infty$. Thus, Migdal's theorem is built into the large N approach [19]. The $1/N$ picture has been called the 'leap to all loops' [2]. Here, in making the leap, we land on Eliashberg's theory, and obtain Migdal's theorem during the trajectory.

Just for completeness, we can proceed and see how the loop-counting works in the contributions for the four-fermion vertex using the double-index notation. Fig. 1(c) shows the contributions in terms of the box-vertex $\tilde{u}$ obtained after integrating out the phonons. At this point we can immediately apply the results of [2] and be done. Alternatively, if the phonons are kept, we open the box-vertex and the diagrams of Fig. 1 are represented by the ones in Fig. 5. The first two diagrams in the series are the tree-level ones, the next three are contained in the box-vertex BCS diagram, and the last ones are examples of diagrams that are contained in the box-vertex ZS diagram.

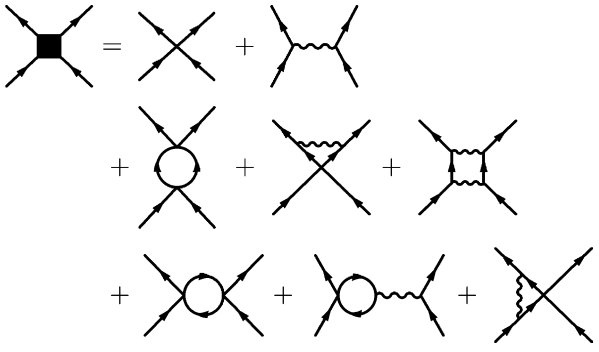

Fig. 5. Corrections to $\Gamma(u)$ corresponding to opening the box-vertex of Fig. 1(c).

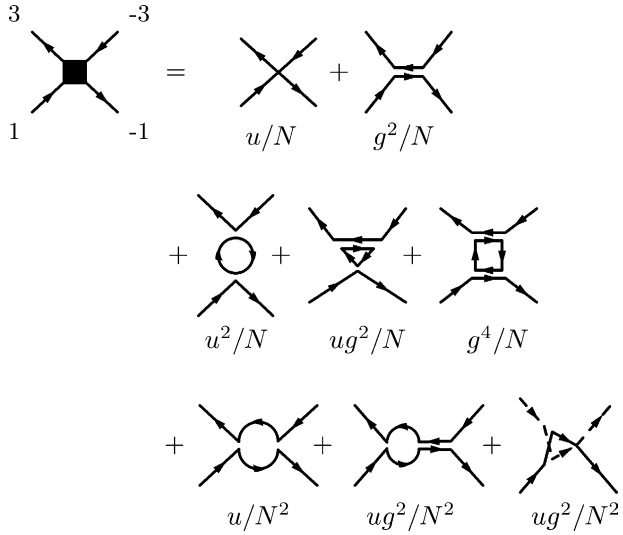

Fig. 6. Contributions to the Cooper channel four-point vertex using the two-fermion representation for the phonon propagator. The presence of an internal closed loop can be easily identified and each one represents a factor N. The dashed line in one of the diagrams is equivalent to a solid line and was introduced just for clarity.

We can now simply redraw the diagrams following the double-index prescription. This is shown in Fig. 6 for the Cooper channel, i.e. incoming electrons with momenta k_1 and $-k_1$ and outgoing electrons with momenta k_3 and $-k_3$. The interaction term goes as $1/N$. The BCS contributions are of the same order, and as expected, the ZS contributions are higher order in $1/N$.

4. Conclusions

We have developed an asymptotically exact RG method that takes into account electron–electron and electron–phonon interactions in an unbiased way. The inclusion of electron–phonon interactions leads to more energy scales in the problem (u, g, $\omega_E \ll \Lambda_0$) and also to retardation effects. It is interesting to note that, for the starting action at λ_0, all that is required is that all the other scales are much smaller than the energy cut-off. They can, however, have different relative magnitudes. This is the reason why we could apply it not only for small λ ($g \ll \omega_E$) but also for $\lambda \gg 1$ ($g \gg \omega_E$).

Our procedure can be used for any Fermi surface geometry and for any number of scattering channels (forward, charge and spin density wave, etc) and therefore allows for the study of the competition between scattering channels [10]. In this work we focused entirely on the problem of the superconducting instability. For a circular Fermi surface it is shown that the Eliashberg's theory of strongly coupled superconductors is asymptotically exact (in the same sense the Landau's theory of the Fermi liquid is asymptotically exact) and that Migdal's theorem follows from the RG. Finally, our procedure allows for a new way to investigate superconductivity in metals and the competition between different instabilities when both electron–electron and electron–phonon are at play.

Acknowledgements

We thank J. Carbotte, A. Chubukov, C. Chamon, J. B. Marston, G. Murthy, and M. Silva-Neto for illuminating discussions and the Aspen Center for Physics for its hospitality during the early stages of this work. A. H. C. N. was supported by NSF grant DMR-0343790. R. S. was supported by NSF grant DMR-0103639.

References

[1] S.-W. Tsai, A.H. Castro Neto, R. Shankar, D.K. Campbell, Renormalization-group approach to strong-coupled superconductors, cond-mat/0406174.
[2] R. Shankar, Rev. Mod. Phys. 68 (1994) 129.
[3] X.J. Zhou, et al., cond-mat/0405130.
[4] L. Pintschovius, H. Rietschel, T. Sasaki, H. Mori, S. Tanaka, N. Toyota, M. Lang, F. Steglich, Europhys. Lett 37 (1997) 627.
[5] R.H. McKenzie, Science 278 (1997) 820.
[6] H.J. Choi, M.L. Cohen, S.G. Louie, Physica C385 (2003) 66.
[7] A. Deppeler, A.J. Millis, Phys. Rev. B 65 (2002) 224301.
[8] J.E. Han, O. Gunnarsson, V.H. Crespi, Phys. Rev. Lett. 90 (2003) 167006.
[9] See e.g. D.J. Amit, Field Theory, The Renormalization Group, and Critical Phenomena, World Scientific, 1984.
[10] S.-W. Tsai, et al., unpublished.
[11] G.M. Eliashberg, Zh. Eksp. Teor. Fiz. 38 (1960) 966; G.M. Eliashberg, Sov. Phys. JETP 11 (1960) 696.
[12] SeeJ.P. Carbotte, Rev. Mod. Phys. 62 (1990) 1027 and references therein.
[13] W.L. McMillan, Phys. Rev. 167 (1968) 331.
[14] P. Morel, P.W. Anderson, Phys. Rev. 125 (1962) 1263.
[15] P.B. Allen, R.C. Dynes, Phys. Rev. B 12 (1975) 905.
[16] C.R. Leavens, J.P. Carbotte, Can. J. Phys. 49 (1971) 724.
[17] A.B. Migdal, Zh. Eksp. Teor. Fiz. 34 (1958) 1438; A.B. Migdal, Sov. Phys. JETP 7 (1958) 996.
[18] G.T. t'Hooft, Nucl. Phys. 72 (1974) 461.
[19] Adifferent finite large N approach for the spin-fermion model has been proposed by Ar. Abanov, A. Chubukov, A.M. Finkelstein, Europhys. Lett. 54 (2001) 488 with similar conclusions.
[20] D. Zanchi, H.J. Schulz, Phys. Rev. B 61 (2000) 13609; C.J. Halboth, W. Metzner, Phys. Rev. B 61 (2000) 7364; S.-W. Tsai, J.B. Marston, Can. J. Phys. 79 (2001) 1463.